A core of functionally complementary bacteria colonizes oysters in Pacific Oyster Mortality Syndrome

Aude Lucasson, Xing Luo, Shogofa Mortaza, Julien de Lorgeril, Eve Toulza, Bruno Petton, Jean-Michel Escoubas, Camille Clerissi, Lionel Dégremont, Yannick Gueguen, et al.

A core of functionally complementary bacteria colonizes oysters in Pacific Oyster Mortality Syndrome.

Aude Lucasson[1#], Xing Luo[2#], Shogofa Mortaza[2#], Julien de Lorgeril[1], Eve Toulza[1], Bruno Petton[3], Jean-Michel Escoubas[1], Camille Clerissi[4], Lionel Dégremont[5], Yannick Gueguen[1], Delphine Destoumieux-Garzón[1], Annick Jacq[2,&] and Guillaume Mitta[1,&]

[1] IHPE, Université de Montpellier, CNRS, Ifremer, Université de Perpignan Via Domitia, Place E. Bataillon, CC080, 34095 Montpellier, France and 58 Avenue Paul Alduy, 66860 Perpignan, France

[2] Université Paris-Saclay, CEA, CNRS, Institute for Integrative Biology of the Cell (I2BC), 91198, Gif-sur-Yvette, France

[3] Ifremer, LEMAR UMR 6539, UBO, CNRS, IRD, Ifremer, 11 presqu'île du vivier, 29840 Argenton-en-Landunvez, France

[4] PSL Université Paris: EPHE-UPVD-CNRS, USR 3278 CRIOBE, Université de Perpignan, 52 Avenue Paul Alduy, 66860 Perpignan Cedex, France

[5] Ifremer, SG2M, LGPMM, Avenue du Mus de Loup, 17930 La Tremblade, France

#These authors contributed equally: Aude Lucasson, Xing Luo and Shogofa Mortaza

& These two last authors contributed equally: Annick Jacq and Guillaume Mitta. Correspondence and requests for materials should be addressed to A.J. (email: annick.jacq@universite-paris-saclay.fr) or to G.M. (email: mitta@univ-perp.fr)

ABSTRACT

The Pacific oyster *Crassostrea gigas* is one of the main cultivated invertebrate species around the world. Since 2008, oyster juveniles have been confronted with a lethal syndrome, Pacific Oyster Mortality Syndrome (POMS). The etiology of POMS is complex. Recently, we demonstrated that POMS is a polymicrobial disease. It is initiated by a primary infection with the *herpesvirus* OsHV-1 µ Var, and evolves towards a secondary fatal bacteremia that is enabled by the oyster's immunocompromised state. In the present article, we describe the implementation of an unprecedented combination of metabarcoding and metatranscriptomic approaches to show that the sequence of events in POMS pathogenesis is conserved across infectious environments and susceptible oyster genetic backgrounds. We also identify a core colonizing bacterial consortium which, together with OsHV-1 µ Var, forms the POMS pathobiota. This bacterial core is characterized by highly active global metabolism and key adaptive responses to the within-host environment (e.g. stress responses and redox homeostasis). Several marine gamma proteobacteria in the core express different and complementary functions to exploit the host's resources. Such cross-benefits are observed in colonization-related functions, and reveal specific strategies used by these bacteria to adapt and colonize oysters (*e.g.* adhesion, cell defense, cell motility, metal homeostasis, natural competence, quorum sensing, transport, and virulence). Interdependence and cooperation within the microbial community for metabolic requirements is best exemplified by sulfur metabolism, which is a property of the pathobiota as a whole and not of a single genus. We argue that this interdependence may dictate the conservation of the POMS pathobiota across distinct environments and oyster genetic backgrounds.

INTRODUCTION

Introduced from Asia to a broad range of countries, *Crassostrea gigas* has become one of the world's main cultivated species. Since 2008, juvenile stages of *C. gigas* have suffered massive mortality events, especially in France [1]. In subsequent years, this so-called Pacific Oyster Mortality Syndrome (POMS) [2] has become panzootic. POMS has been observed in all coastal regions of France [3-5] and numerous other countries worldwide [6-11].

This situation has promoted a research effort that has revealed a series of factors contributing to the disease, including infectious agents that interact with seawater temperature and oyster genetics [12-17]. Dramatic POMS mortality events have coincided with the recurrent detection of *Ostreid herpesvirus* variants in moribund oysters [3-5]. The involvement of other etiological agents has also been suspected. In particular, bacterial strains of the genus *Vibrio* have been shown to be associated with the disease [18, 19]. Recently, integrative molecular approaches performed on susceptible and resistant families of oysters have revealed the complex etiology of POMS [20, 21]. These studies demonstrated that infection by *Ostreid herpesvirus* type 1 µVar (OsHV-1) is a critical step in POMS pathogenesis. OsHV-1 leads to an immunocompromised state by altering hemocyte physiology. This results in dysbiosis and bacteremia, which ultimately results in oyster death [20]. Several bacterial genera are involved in this secondary infection [20]; one of them *(Vibrio)* was found to include opportunistic pathogens that cause hemocyte lysis [21]. This observation occurred in a specific infectious environment in French Brittany [20]. Whether the observed mechanisms of POMS pathogenesis are conserved in other infectious environments remains unknown. Also of importance, *Vibrio* species are not the only bacteria that colonize oyster tissues during the secondary bacterial infection. Several bacterial genera, including *Arcobacter*, *Marinobacterium*, *Marinomonas*, and *Psychrobium* are also found to massively colonize oysters [20]. The mechanisms underlying the colonizing capacity of these species remain to be elucidated.

In the present study, we investigated whether POMS pathogenesis is conserved across environments, and which biological functions are expressed by the bacterial consortia that causes oyster death. We compared pathogenesis in oyster biparental families that display contrasting phenotypes (resistant or susceptible to POMS) in two infectious environments (the Atlantic Bay of Brest environment, and the Mediterranean Thau Lagoon environment). We found that the sequence of events is conserved in both infectious environments: intense viral replication in susceptible oysters, followed by a secondary bacteremia caused by a conserved bacterial consortium that results in oyster death. Using metabarcoding and metatranscriptomics, we identified members of the core colonizing bacterial consortium, and characterized their highly active metabolism and key adaptive responses to the within-host environment. We also identified a series of genus-specific functions required for

colonization, which reveal specific strategies that the core consortium uses to adapt and colonize oysters. Finally, we identified cooperative processes used by the core consortium to meet their metabolic requirements; these processes may dictate the conservation of the core consortium across environments.

METHODS

Production of biparental oyster families

C. gigas families were produced as described in [20, 22]. Briefly, oysters were produced at the Ifremer hatchery in Argenton in March 2015. Three susceptible families (F_{11}, F_{14}, and F_{15}) and three resistant families (F_{21}, $F_{23,}$ and F_{48}) were used as recipients, and 15 families were used as donors. All families were maintained under controlled bio-secured conditions to ensure their specific pathogen-free status. Status was verified by i) the absence of OsHV-1 DNA using qPCR, (see below) and ii) a low *Vibrio* load (~10 cfu/g tissue) on selective culture medium (thiosulfate-citrate-bile salts-sucrose agar) [23]. Oysters remained free of any abnormal mortality throughout larval development, at which time experimental infections were started.

Mesocosm experimental infections

The experimental infection protocol consisted of a cohabitation assay between donors (exposed to pathogens naturally present in the environment) and recipient specific pathogen-free oysters [17, 18]. Details of the experimental infection protocol (e.g. biomass, oyster weight, experimental duration, and tank volume) were as described in [20, 22]. Briefly, donor oysters were deployed at Logonna Daoulas (lat 48.335263, long 4.317922) in French Brittany (Atlantic environment) and at Thau Lagoon (lat 43.418736, long 3.622620) (Mediterranean environment). Oysters were deployed in farming areas during the infectious period, and remained in place until the onset of mortality (< 1%). Donors were then brought back to the laboratory (in Argenton) and placed in tanks, each containing recipient oysters from the three resistant and the three susceptible families. Experimental infections took place in July 2015 and September 2015 for the Atlantic and Mediterranean exposures, respectively. For each

107 experimental infection, mortality rate was monitored, and 10 oysters were sampled in triplicate from
108 each oyster family shucking at 7 time points (0, 6, 12, 24, 48, 60, and 72 hours post-infection). The
109 shell was removed and the whole oyster was flash frozen in liquid nitrogen. Oyster pools were ground
110 in liquid nitrogen in 50 ml stainless steel bowls with 20mm diameter grinding balls (Retsch MM400
111 mill). The powders obtained were stored at -80°C prior to RNA and DNA extraction.

112 **DNA extraction and quantification of OsHV-1 and total bacteria.**

113 DNA extraction was performed as described in [20] using the Nucleospin tissue kit (Macherey-Nagel).
114 DNA concentration and purity were checked with a NanoDrop One (Thermo Scientific).
115 Quantification of OsHV-1 and total bacteria were performed using quantitative PCR (qPCR) with a
116 Roche LightCycler 480 Real-Time thermocycler (qPHD-Montpellier GenomiX platform, Montpellier
117 University, France). Absolute quantity of OsHV-1 was calculated by comparing the observed Cq
118 values to a standard curve of the OsHV-1 DNA polymerase catalytic subunit (AY509253)
119 amplification product cloned into the pCR4-TOPO vector (Invitrogen). Relative quantification of total
120 bacteria 16S rDNA gene was calculated by the $2^{-\Delta\Delta Cq}$ [24] method with the mean of the measured
121 threshold cycle values of two reference genes (*Cg-BPI*, GenBank: AY165040 and *Cg-actin*, GenBank:
122 AF026063) (de Lorgeril, Lucasson et al. 2018).
123
124 **Analyses of bacterial microbiota**

125 Bacterial metabarcoding was performed using 16S rRNA gene amplicon sequencing. Libraries were
126 generated using the Illumina two-step PCR protocol targeting the V3-V4 region [25]. A total of 252
127 libraries (six families × seven sampling time points × three replicates × two infectious environments)
128 were paired-end sequenced with a 2 × 250 bp read length at the Genome Quebec platform on a MiSeq
129 system (Illumina) according to the manufacturer's protocol. A total of 41,012,155 pairs of sequences
130 were obtained. Metabarcoding data was processed using the FROGS pipeline [26]. Briefly, paired
131 reads were merged using FLASH [27]. After cleaning steps and singleton filtering, 26,442,455
132 sequences were retained for further analyses. After denoising and primer/adapter removal with
133 cutadapt, clustering was performed using SWARM, which uses a two-step clustering algorithm with a

threshold corresponding to the maximum number of differences between two Operational Taxonomic Units (OTU) (denoising step d = 1; aggregation distance = 3) [28]. Chimeras were removed using VSEARCH [29]. Resulting OTUs were annotated using Blast+ against the Silva database (release 128).

Bacterial metatranscriptomic analysis

Powder obtained from the frozen oysters was resuspended in Trizol, and total RNA was extracted using a Direct-zol™ RNA Miniprep kit. Polyadenylated mRNAs (*i.e.* oyster mRNAs) were removed using a MICROB*Enrich*™ Kit (Ambion). cDNA oriented sequencing libraries were prepared as described in [21] using the Ovation Universal RNA-Seq system (Nugen). Library preparation included steps to remove oyster nuclear, mitochondrial, and ribosomal RNAs, as well as bacterial rRNAs [21]. A total of 36 libraries (three families × two sampling timepoints × three replicates × two infectious environments) were sequenced by the Fasteris company (Switzerland, https://www.fasteris.com) in paired-end mode (2 × 150 bp) on an Illumina HiSeq 3000/4000 to obtain 200-300 million clusters per sample (**Supplementary Table 1**).

Figure S1 presents a schematic of data processing. Raw Illumina sequencing reads from 72 fastq files (R1 and R2) were trimmed using Trimmomatic v0.38, and rRNA reads (both eukaryotic and bacterial) were removed using Sortme RNA v2.1b with the rRNA Silva database (release 128). At this stage, about 9% of reads were removed, underscoring the efficiency of experimental rRNA removal during library preparation (**Supplementary Figure 1**).

To further enrich bacterial sequences, reads were successively mapped by Bowtie2 [30] on a multifasta file containing *Crassostrea gigas* genome sequence v9, complemented by *C. gigas* EST (available from NCBI), and a multifasta file containing the sequences of OsHV-1 (present in diseased oysters) and other viral sequences previously associated with bivalves [31]. Unmapped reads, which represented 4-10% of the starting reads (depending on conditions) were retained for further analysis (**Supplementary Table 1**). After a new filtering step using Trimmomatic, all remaining reads corresponding to the 36 samples were pooled (516,786,580 reads, 36-150 nt) and assembled using Trinity v2.3.2 in paired-end mode to build a reference metatranscriptome (1,091,409 contigs, 201 –

15,917 nt). The resulting metatranscriptome was further annotated using Diamond BlastX against the NCBI nr protein database [32]. 48.4 % of the contigs aligned with a protein in the database, and were further assigned to a taxon using Megan 6-LR Community Edition [33]. Sequences were annotated at different taxonomic levels from species to phylum. Out of the 1,091,409 contigs, 352,473 contigs aligned with bacterial proteins by BlastX with an E-value $\leq 01^{e}$-06.

Each protein was assigned to 31 functional categories (**Supplementary Table 2**). Out of the 352,473 best hits, 74,015 were annotated as "hypothetical", "unknown", or "unnamed", and were assigned to the category "Unknown function". The remaining hits corresponded to 15,504 different protein names that were manually assigned to one of the 30 remaining functional categories.

Quantification of gene expression and data normalization

For each of the 36 samples used for the assembly of the metatranscriptome, reads were mapped back onto the metatranscriptome by Bowtie2 in paired-end mode. Raw counts per features (*i.e.* per contig) were computed using HTseq-Count [34]. For each contig, and for each sample, raw counts were normalized to TPM (Transcripts per Kilobase / Million = Mapped reads / Length of contig (kb) / Scaling factor with Scaling factor = total reads in a sample / 1,000,000), which corrects for contig length and differences in read number in the different samples. **Supplementary Table 3** presents a complete list of contigs, their length, the encoded feature annotation, and the TPM value of the feature in each sample. In many cases, one protein could be encoded by several contigs, either because gene assembly into a contig was incomplete, or because of the existence of contig isoforms. Altogether, the 352,473 contigs encoded 225,965 unique proteins.

When analyzing the functional enrichment in the seven genera that predominated in the microbiota of diseased oysters (see **Results** section), contigs that encoded the same protein were merged into a single feature/protein, and their expression levels were summed. The expression level of a category was calculated by summing up the expression level of all the proteins assigned to the category. In addition, expression values were normalized from TPM to a value corrected for the relative proportion of the genus activity in the sample such that the ratio of the average normalized expression level of the three replicates for a given functional category in two conditions (*i.e.* T60 or 72 vs T0) reflected a

specific enrichment (Enrichment Factor or EF) of the function, rather than a general increase of the genus in the population. First, a pseudo count of one read was added to each gene in each condition/replicate, and the resulting counts were normalized by dividing by the total number of counts of the genus in a given condition/replicate, then multiplying by 10,000. For a given function/protein or functional category, an enrichment factor (EF) between the two conditions (i.e. T60 or T72 vs T0) was further defined as the ratio of the average normalized expression level of the three replicates at T60 or 72 over the average expression level at T0.

Statistical analyses

Survival curves were used to determine differential mortality kinetics between oyster families with the non-parametric Kaplan-Meier test (Mantel–Cox log-rank test, $p < 0.05$, GraphPad_Prism 6.01). For OsHV-1 and total bacteria quantifications, significant differences between resistant and susceptible oyster families were determined using the non-parametric Mann Whitney test ($p < 0.05$, GraphPad_Prism 6.01). For bacterial metabarcoding, statistical analyses were performed using R v3.3.1 (http://www.R-project.org, [35]). Principal coordinate analysis (PCoA, "phyloseq") on a Bray-Curtis distance matrix (ordinate, "phyloseq") was performed to determine dissimilarities between samples. Multivariate homogeneity of group dispersions was tested between bacterial assemblages of the six oyster families using 999 permutations (permutest, betadisper, "vegan"). DESeq2 ("DESeq", [36]) from the OTUs to the higher taxonomic ranks was used to identify candidate taxa whose abundance changed between the initial and final time points of the experiment. The abundance of a bacterial taxon was considered significantly modified when the adjusted p-value for multiple testing with the Benjamini-Hochberg procedure, which controls the false discovery rate (FDR), was $<$ 0.05. Heatmaps of significant genera were computed using relative abundances and the heatmap.2 function "ggplots" [37]. For bacterial metatranscriptomics, significant differences in expression between two conditions (i.e. T60 or T72 vs T0) were assessed by a paired Student's t-test ($p < 0.05$).

Data availability

Metabarcoding and RNAseq sequence data will be made available through the SRA database (BioProject accession number PRJNA423079 with SRA accession SUB7738644 for bacterial metabarcoding and SUB8110348 for Bacterial metatranscriptomic). Other data generated from this study are included in the published version of this article and its supplementary files.

RESULTS

Primary OsHV-1 infection and secondary bacteremia are conserved in POMS, independent of the infectious environment

Six *C. gigas* families were subjected to two experimental infections that mimicked disease transmission in the wild. We previously reported high variability in the dynamics of mortality and percentage survival of oyster families confronted with an Atlantic infectious environment. Specifically, the F11, F14, and F15 families were highly susceptible (survival rate < 4% after 330h) to POMS, whereas the F21, F23, and F48 families were highly resistant (survival rate > 82% after 330h) [20]. Similar results were obtained in the present study when the same oyster families were confronted with a Mediterranean infectious environment: families F11, F14, and F15 were susceptible (survival rates < 9%), whereas families F21, F23, and F48 were resistant (survival rates > 88%) (**Figure 1**). Thus, these oyster families displayed similar phenotypes when confronted with two different infectious environments (Mantel-Cox log-rank test, $p < 0.0001$ for each comparison of resistant *vs.* susceptible oyster families). Susceptible and resistant oyster families are hereafter referred to as S (S_{F11}, $S_{F14,}$ and S_{F15}) and R (R_{F21}, R_{F23}, and R_{F48}), respectively.

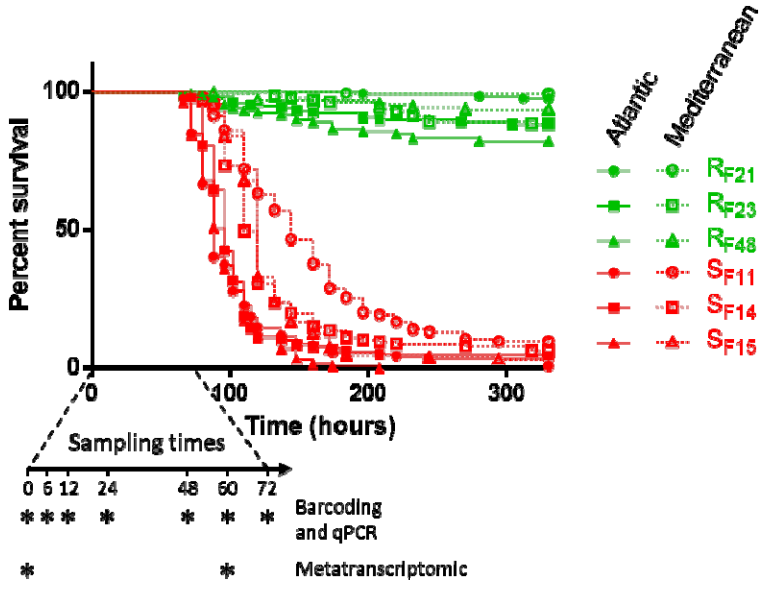

Figure 1: Kaplan-Meier survival curves of oyster biparental families confronted with two different infectious environments. Resistant oyster families (R_{F21}, R_{F23}, and R_{F48}) are presented in

green, and susceptible oyster families (S_{F11}, S_{F14}, and S_{F15}) are presented in red. At each time point (indicated by asterisks on the arrow), 10 oysters were sampled 3 triplicates from each family in each tank for barcoding, qPCR, and metatranscriptomic analysis. Data for the Atlantic infectious environment are extracted from [20] and shown for comparison.

We next compared pathogenesis between the two infectious environments by monitoring OsHV-1 load, microbiota dynamics, and bacterial abundance in the three resistant and three susceptible oyster families (**Figure 2**). OsHV-1 DNA was detected in all families, regardless of whether they were confronted with the Atlantic or Mediterranean infectious environment (**Figure 2a)**. However, very intense viral replication occurred only in the susceptible oyster families: viral DNA loads were 2 to 3 logs higher than in resistant oysters at 24 h (**Figure 2a**).

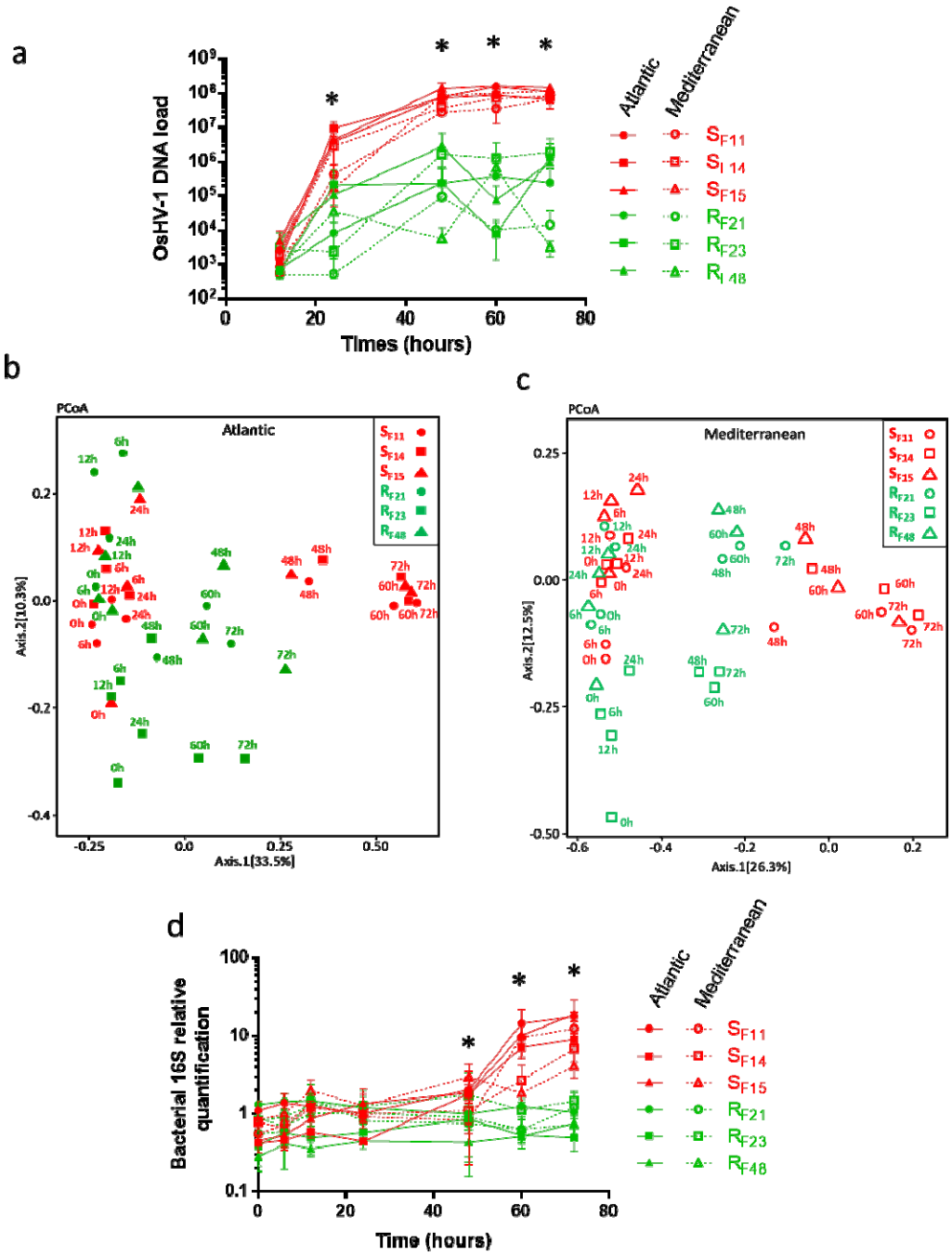

250

251 **Figure 2: Primary OsHV-1 infection, bacterial dysbiosis, and secondary bacteremia are**
252 **conserved in different infectious environments. (a)** Early and intense replication of OsHV-1 µVar
253 occurs in susceptible oysters (red), but not resistant oysters (green), confronted with either the Atlantic
254 or the Mediterranean infectious environment. OsHV-1 load was quantified by qPCR and expressed as
255 Viral Genomic Units per ng of oyster DNA (log scale) during experimental infections. Asterisks
256 indicate significant differences between susceptible and resistant oyster families (Mann Whitney test,
257 $p < 0.05$). **(b-c)** Principal coordinate analysis (PCoA) plot of the microbiota for susceptible (red) and
258 resistant (green) oyster families confronted with each infectious environment. Dispersion of oyster
259 families according to the Bray-Curtis dissimilarity matrix (beta diversity) in **(b)** Atlantic and **(c)**

Mediterranean infectious environments. **(d)** Temporal dynamics of total bacteria in susceptible (red) and resistant (green) oyster families confronted with two different infectious environments. Total bacterial quantification based on qPCR amplification of the V3-V4 region of the 16S rRNA gene during experimental infections. Asterisks indicate significant differences between susceptible and resistant oyster families (Mann Whitney test, $p < 0.05$). Data from the Atlantic infectious environment in panels (a) and (d) are extracted from [20] for comparison.

The dynamics of the oyster microbiota were studied in the six oyster families by monitoring bacterial community composition using 16S rRNA gene metabarcoding over the first 3 days of both experimental infections. A total of 45,686 bacterial OTUs were obtained from the 252 samples and affiliated at different taxonomic ranks (**Supplementary Table 4**). Sufficient sequencing depth was confirmed by species richness rarefaction curves (**Supplementary Figure 2**). Changes in microbiota composition were greater in susceptible oysters than in resistant oysters at all taxonomic ranks (**Supplementary Figure 3**). Indeed, for the Atlantic infectious environment, 52, 43, and 54 OTUs significantly differed (in terms of relative proportion between the start and end of the experiment) in susceptible oysters S_{F11}, S_{F14} and S_{F15}, respectively; only 1, 11, and 9 OTUs significantly differed in resistant oysters R_{F21}, R_{F23} and R_{F48}, respectively (**Supplementary Table 5**). The same trend was observed in the Mediterranean infectious environment. 11, 47, and 43 OTUs significantly differed in S_{F11}, S_{F14} and S_{F15}, respectively, as opposed to 2, 8, and 6 OTUs in R_{F21}, R_{F23} and R_{F48}, respectively.

PCoA on a Bray-Curtis dissimilarity matrix (beta diversity) revealed higher microbiota dispersion in susceptible oyster families than in resistant families in both infectious environments (multivariate homogeneity of groups dispersion, d.f. = 1; $p = 0.016$ and $p = 0.020$ for Atlantic and Mediterranean environments, respectively) (**Figure 2b and 2c**). This disruption of the bacterial community structure occurred in susceptible oysters between 24 h and 48 h, concomitantly with the active replication of OsHV-1. In addition, susceptible oyster families displayed a significantly greater bacterial load than resistant oysters when confronted with either the Atlantic or the Mediterranean infectious environment (Mann Whitney test, $p < 0.05$; **Figure 2d**). This increase started at 60 h and continued to until the end of the experiment (72 h). Total bacterial abundance in susceptible oysters was more than 5-fold higher at 72 h than at T0, which indicated bacterial proliferation. In contrast, total bacterial load remained stable in resistant oysters.

A core of bacterial genera colonizes oysters during secondary bacterial infection in POMS

All bacterial genera that changed significantly in abundance during the two experimental infections (Atlantic and Mediterranean) in susceptible oyster families are reported in **Supplementary Table 5** (DESeq2, adjusted $p < 0.05$). We focused on genera representing > 2% of the bacteria in at least one sample for each susceptible oyster family confronted with each infectious environment (**Figure 3)**. In the Atlantic infectious environment, the corresponding OTUs represented a total of 4%, 0.8%, and 46% of total bacteria at the beginning of the experiment (T0), as opposed to 73%, 75%, and 72% at 72 h for S_{F11}, S_{F14}, and S_{F15}, respectively (**Supplementary Table 5**). In the Mediterranean infectious environment, these OTUs increased from 2%, 6%, and 7% at T0 to 47%, 56%, and 56% at 72 h for S_{F11}, S_{F14}, and S_{F15}, respectively. Nine to twenty genera increased significantly in abundance between T0 and 72 h. Ten genera (*Arcobacter*, *Cryomorphaceae*, *Marinobacterium*, *Marinomonas*, *Proxilibacter*, *Pseudoalteromonas*, *Psychrilyobacter*, *Psychrobium*, *Psychromonas*, and *Vibrio*) were common to almost all (5 of 6) susceptible oyster families and both infectious environments (**Figure 3**). Most of the remaining genera (*Aquibacter*, *Aureivirga*, *Fusibacter*, *Neptunibacter*, *Peredibacter*, *Pseudofulbibacter*) were shared by at least two families in one infectious environment. One genera (*Salinirepens*) increased significantly in all susceptible oysters in the Atlantic infectious environment only. These results show that a core of bacterial genera colonizes oysters during the POMS secondary bacterial infection, independent of the infectious environment. In resistant oyster families, several taxa also vary significantly in abundance over time. Most of these taxa are the same taxa identified in susceptible oyster families (**Supplementary Figure 4)**, but they are present in lesser quantities. These taxa represent between 4% to 23% of the reads sequenced at 72h in resistant oysters, whereas they represent 47% to 75% of the reads sequenced in susceptible oysters (**Supplementary Table 5**).

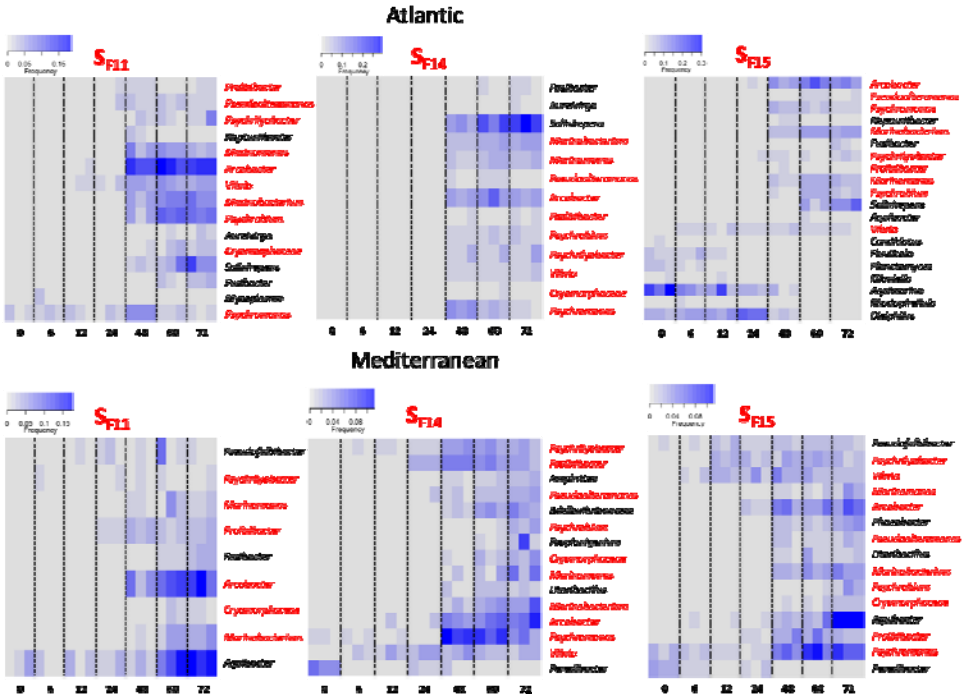

Figure 3: **Heatmaps of bacterial genera that changed significantly in abundance over the course of infection in susceptible oysters (S_{F11}, S_{F14}, and S_{F15}) in the Atlantic and Mediterranean infectious environments.** Analyses were performed at the genus level. Only genera that changed significantly in abundance (DESeq2, adjusted $p < 0.05$) and had a relative proportion greater than 2% in at least one sample are shown. Increased intensity of color (blue) represents increased relative abundance. Genera that are consistently modified in 5 out of the 6 conditions (3 families and 2 infectious environments) are in red.

Seven genera are responsible for most bacterial gene expression in diseased oysters

To understand the colonization success of certain genera, we analyzed the gene expression of the colonizing microbiota. As described in the **Methods** section, we used metatranscriptomics to determine the functional mechanisms underlying colonization for different bacterial genera in the three different oyster genetic backgrounds and two different infectious environments. RNAseq was performed after removal of rRNA, oyster mRNA, and mitochondrial RNA using custom probes. We sequenced the remaining RNA of the susceptible families S_{F11}, S_{F14}, and S_{F15}, in both the Atlantic and Mediterranean infectious environments, at T0 and just before oyster mortality occurred (*i.e.* at 60 h and 72 h for the Atlantic and the Mediterranean infectious environments, respectively). Three biological replicates were analyzed for each condition, corresponding to a total of 36 biological samples. After removal of the remaining non-bacterial and ribosomal reads, we assembled and

annotated a reference metatranscriptome. We aligned the translated contigs with the NCBInr protein database, and used MEGAN for taxonomic assignments. We obtained 352,473 contigs that aligned with bacterial proteins with an e-value ≤ 10^{-6}. In many cases, a single protein could be encoded by several contigs, either because the gene was not fully assembled or because of contig isoforms. In total, our assembled metatranscriptome encoded 225,965 unique proteins. These protein were functionally and taxonomically annotated, and their expression level was determined for each condition. Further analyses were restricted to proteins assigned at the genus or species levels.

To analyze the contribution of each genus to the overall bacterial gene expression, we added the level of expression of all proteins assigned to a given genus (measured in Transcripts Per Million, or TPM). We focused on genera that contributed to more than 2% of total gene expression in at least one oyster sample (**Figure 4**).

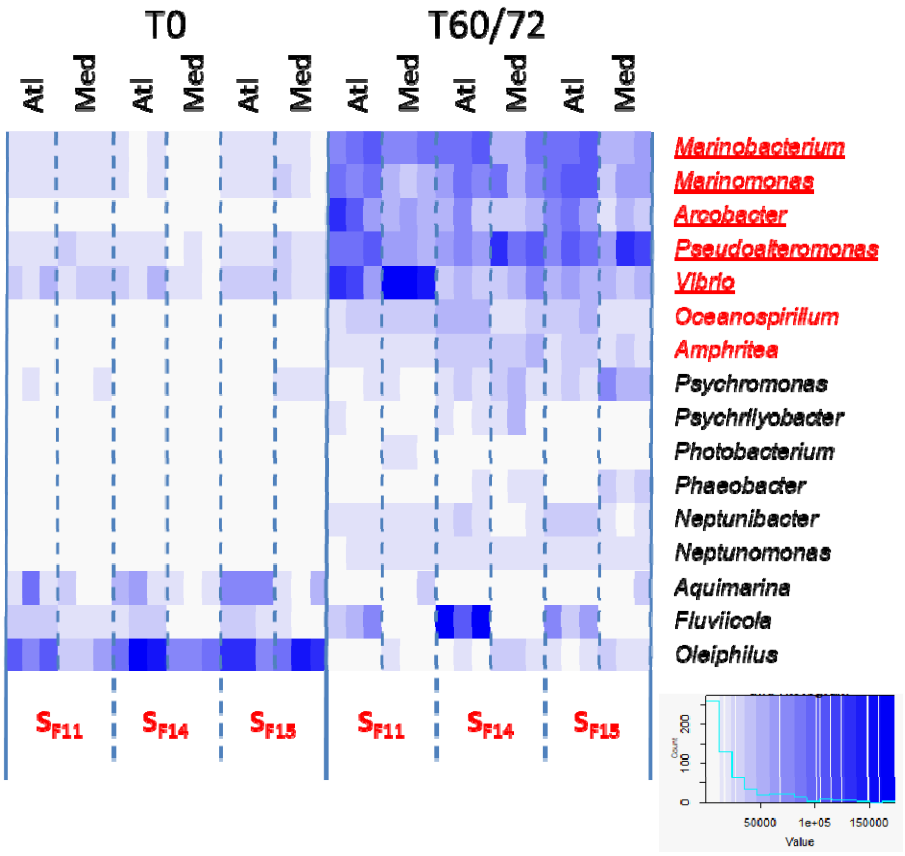

Figure 4: Heatmap of transcriptional activity of bacterial genera in susceptible oyster families (S_{F11}, S_{F14}, and S_{F15}) in the two infectious environments before infection and in diseased oysters. For each condition, results of the three replicates are shown. Increased color intensity (blue) indicates

increased relative activity of the genus. Genera shown contributed at least 2% of the total transcriptional activity in at least one sample of diseased oysters. Bacterial genera that were overrepresented according to metatranscriptomics alone for all conditions in the diseased oysters are in red, while genera that were overrepresented according to both metabarcoding and metatranscriptomics are underscored. (Atl: Atlantic, Med: Mediterranean, T0: before infection, T60/72: diseased)

Seven genera were consistently found to contribute the majority of transcriptomic activity in diseased oysters, displaying a strong increase in the number of transcripts compared to healthy oysters. *Amphitrea, Arcobacter, Marinobacterium, Marinomonas, Oceanospirillum, Pseudoalteromonas,* and *Vibrio* were together responsible for up to 40% of the total bacterial transcriptomic activity detected just before the onset of oyster mortality. All are Gram-negative bacteria, and 6 out of 7 are Gammaproteobacteria. Of the six Gammaproteobacteria, *Amphitrea, Marinobacterium, Marinomonas* and *Oceanospirillum* belong to the same family (Oceanospirillaceae) and order (Oceanospirillales). *Arcobacter* belongs to the class Epsilonproteobacteria. The genus *Fluviicola,* which belongs to the phylum *Bacteroidetes,* presented an increase of transcriptomic activity in the Atlantic infectious environment only. Finally, the genus *Oleiphilus (*order Oceanospirillales), was represented at a maximum level of 1.9 % in diseased oysters.

These results indicate that a limited number of genera participate in the secondary bacteremia that occurs in POMS. These genera are remarkably conserved between the different susceptible oyster families and infectious environments. We therefore focused on these seven genera for additional study.

Secondary bacterial colonizers display genus-specific strategies

We focused on the late phase of the infection process in our examination of the functions underpinning successful colonization by the seven genera discussed above. 31 functional categories were defined, and each transcript-encoded protein was assigned to one of them (**Supplementary Table 2**). For each genus and each category, an enrichment factor (EF) was calculated relative to the general increase of the genus in the bacterial population (See Materials and Methods for details, **Figure 5**).

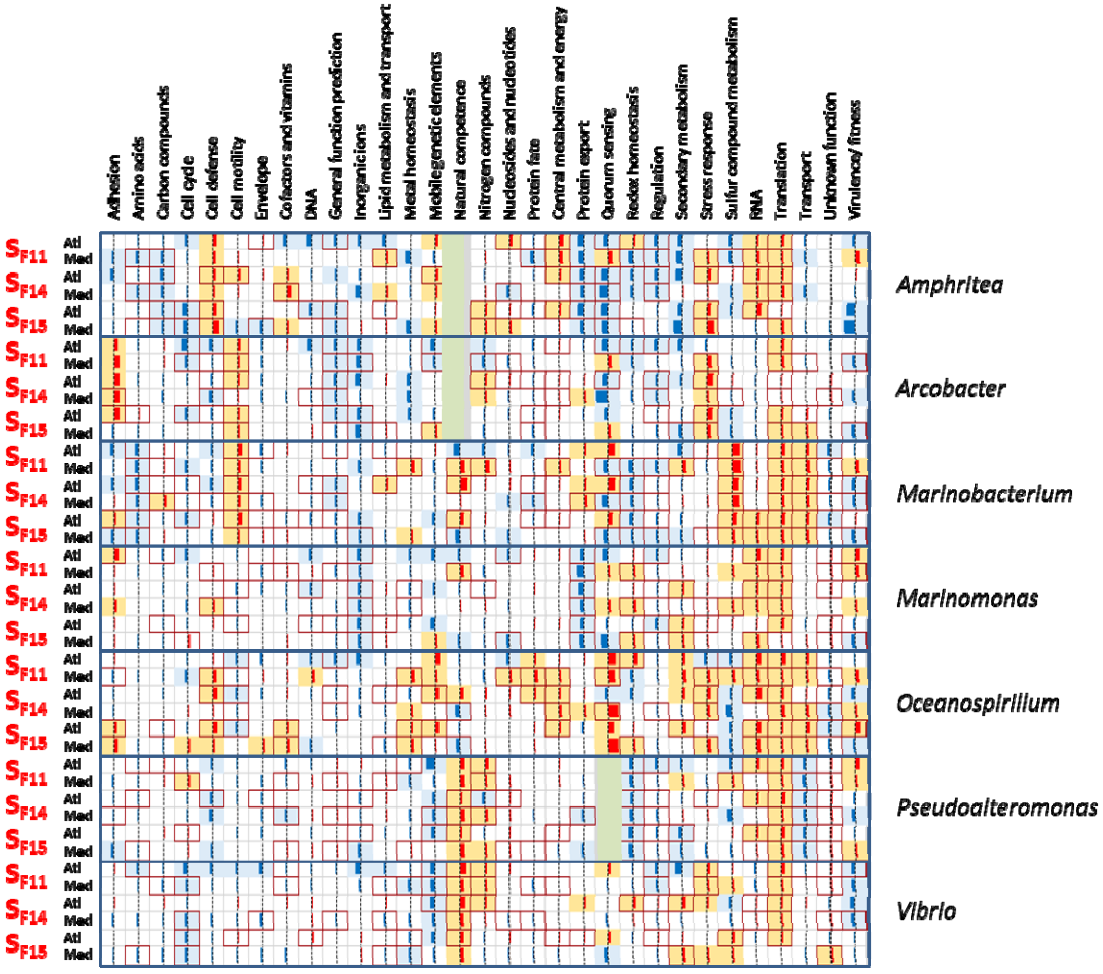

Figure 5. **Functional enrichment between T0 and the onset of oyster mortality.** The enrichment factor (EF) was calculated for each functional category for the seven most active genera present in all families and both environments. Each overrepresented (red) or underrepresented (blue) functional category is indicated by a bar with a width proportional to log2(EF). Red boxes around bars indicate $p \leq 0.05$ (Student's t-test). Green-filled cells indicate functional categories with no gene expression (genes absent from the genome in that genus or not expressed in any conditions). Light blue-filled cells indicate values lower than the 20th percentile, while yellow-filled cells indicate values higher than the 20th percentile.

For all genera except *Arcobacter*, translation and transcription appeared to be globally overrepresented in diseased oysters. Aside from these functions, we found that each colonizing genus displayed a specific pattern of functional enrichment, which was generally conserved across oyster families and environments. For instance, adhesion, cell defense, motility, natural competence, quorum sensing, stress response, and virulence gene expression were either over- or under-represented according to the

391 genus considered. These results suggest that each genus adopts a specific strategy to ensure
392 colonization success.

393

394 **Enriched functions are potentially important for successful colonization**

395 In a global metatranscriptomic analysis, important overrepresented transcripts/subcategories could be
396 hidden by the under-expression of genes classified as being in the same functional categories.
397 Therefore, we next focused our analysis on overrepresented transcripts (listed in **Supplementary**
398 **Table 6**), and identified several overexpressed genes that are likely to contribute to efficient
399 colonization. **Table 1** summarizes the distribution of these overexpressed genes/subcategories within
400 the seven genera.

Table 1. Specific enrichment of selected functions in the seven genera. Overexpression of function/gene in a given genus is indicated by a filled out green cell. E.C. numbers are indicated whenever applicable. Functions that are enriched in all seven genera are in boldface. The relevant information was extracted from supplementary table S6.

Category	Role/pathways	Enriched functions/genes	E.C.. Number	Amphitrea	Arcobacter	Marinobacterium	Marinomonas	Oceanospirillum	Pseudoalteromonas	Vibrio
Cell defense										
	Arsenic detoxification	Arsenate reductase	1.6.5.2			■	■		■	
	Cyanide detoxification	Rhodanese like protein	2.8.1.1			■	■		■	■
	Formaldehyde detoxification	Formaldehyde dehydrogenase, glutathione-independent	1.2.98.1	■		■	■	■		
	Drug resistance	Hydroxyacylglutathione hydrolase	3.1.2.26			■			■	
		S-formylglutathione hydrolase	3.1.2.12			■				
		Aminoglycoside phosphotransferase	2.7.1.-						■	
		RND family efflux transporter					■		■	
		TolC family outer membrane protein		■		■	■		■	
	Hg resistance	MerR family DNA-binding transcriptional regulator							■	
Inorganic ion										
	Calcium transport	Ca2+ transporter				■				
	Potassium transport	K+ transport				■		■		
	Sodium transport	Na+/H+ antiporter NhaC				■	■			
	Phosphonate utilisation	Alkyl phosphonate utilization PhnA			■	■				
	Pi homeostasis	Phosphonate transporter		■			■			■
		Alkaline phosphatase	3.1.3.1				■			
		Inorganic diphosphatase		■		■				
		PhoH (Pi starvation)		■			■	■	■	
		Pi transport						■		
		Polyphosphate kinase 2	2.7.4.1			■			■	
	Selenate transport	Selenate transporter			■					
Metal homeostasis										
	Iron homeostasis	Fe(3+) ABC transporter substrate-binding protein			■	■	■		■	
		Ferric iron uptake transcriptional regulator		■		■				
		Imelysin			■	■				
		Bacterioferritin				■	■		■	
		Ferritin						■		
		Siderophore production					■	■		
		TonB-dependent siderophore receptor				■	■		■	
	Copper homeostasis	Copper-translocating P-type ATPase				■	■			
	Metal homeostasis	Heavy metal (Co2+, Zn2+, W...) transporter			■				■	■
		Metal transporter						■	■	
Nitrogen compound metabolism										
	Nitrosative stress	Hydroxylamine reductase	1.7.99.1		■					■
Precursor metabolite and energy production and conversion										
	ATP synthase	ATP synthase	7.1.2.2	■	■	■	■	■	■	■
	Electron transfer	cytochrome C		■	■	■	■	■	■	■
		cytochrome C oxidase	7.1.1.9	■	■	■	■	■	■	■
		Na(+)-translocating NADH-quinone reductase	7.2.1.1	■	■	■	■	■	■	■
		cytochrome B		■	■	■	■			
		cytochrome o ubiquinol oxidase	7.1.1.3				■			
		electron transfer flavoprotein		■		■	■	■	■	
		electron transfer flavoprotein-ubiquinone oxidoreductase	1.5.5.1	■		■		■		
		hybrid-cluster NAD(P)-dependent oxidoreductase					■		■	
		NADH-quinone oxidoreductase	7.1.1.2		■	■		■		
		pyruvate flavodoxin oxidoreductase	1.2.7.1		■					
		ubiquinol oxidase subunit II	7.1.1.7				■			
		ubiquinol-cytochrome c reductase	1.10.2.2	■		■	■			
	Acetyl-CoA biosynthesis	acetate--CoA ligase	6.2.1.1			■	■			■
		pyruvate dehydrogenase	1.9.6.1			■	■	■	■	■
	Anaerobic respiration	fumarate reductase	1.3.5.4		■					
		hydrogenase small subunit	1.12.5.1		■					
		fumarate/nitrate reduction transcriptional regulator Fnr				■			■	

401

Mixed acid fermentation	formate dehydrogenase	1.17.5.3	■	■	■	■	■		
Glycolysis/ gluconeogenesis	phosphoenolpyruvate synthase	2.7.9.2						■	
	pyruvate kinase	2.7.1.40		■	■	■			■
	2,3-bisphosphoglycerate-dependent phosphoglycerate mutase	5.4.2.11			■	■		■	
	fructose-bisphosphatase	3.1.3.11			■			■	
	fructose-bisphosphate aldolase class II	4.1.2.13	■	■	■	■		■	■
	glucose-6-phosphate isomerase	5.3.1.9		■					
	glyceraldehyde-3-phosphate dehydrogenase	1.2.1.12	■	■	■		■		■
	phosphoglycerate kinase	2.7.2.3			■	■	■		
	phosphopyruvate hydratase	4.2.1.11		■		■	■	■	■
	triose-phosphate isomerase	5.3.1.1			■	■		■	■
Glyoxylate shunt	isocitrate lyase	4.1.3.1				■	■	■	■
	CoA ester lyase (malate synthase)	2.3.3.9		■					
	malate synthase	2.3.3.9	■		■	■	■		
L-alanine fermentation	acryloyl-CoA reductase	1.3.1.84		■					
Mixed acid fermentation	acetate kinase	2.7.2.1		■					
	acetoacetyl-CoA reductase	1.1.1.35			■		■	■	
	formate C-acetyltransferase	2.3.1.54							■
	phosphoenolpyruvate carboxylase	4.1.1.49				■			
Nitrate respiration	ferredoxin-type protein NapG	7.1.1.8		■					■
	nitrite reductase	1.7.2.1		■					■
	nitrous-oxide reductase	1.7.2.4			■				
	Ammonia forming cytochrome c nitrite reductase	1.7.2.2		■					■
	Nitrate reductase NapA	1.9.6.1		■	■	■		■	
Pentose phosphate pathway	glucose-6-phosphate dehydrogenase	1.1.1.49						■	
	NADP-dependent phosphogluconate dehydrogenase	1.1.1.44				■			
	ribose-5-phosphate isomerase RpiA	5.3.1.6			■			■	
	ribulose-phosphate 3-epimerase	5.1.3.1	■						
	transaldolase	2.2.1.2						■	
Photosynthesis	phosphoribulokinase	2.7.1.19						■	
PRPP biosynthesis	ribose-phosphate pyrophosphokinase	2.7.6.1	■		■	■	■	■	■
Respiration	Lactate dehydrogenase or related 2-hydroxyacid dehydrogenase	1.1.-.-			■				
	Ldh family oxidoreductase	1.1.5.12			■	■			
	Aerobic respiration control protein arcA								■
TCA cycle	2-oxoglutarate dehydrogenase	1.2.4.2	■		■	■	■	■	■
	2-oxoglutarate synthase	1.2.7.3		■					
	aconitate hydratase	4.2.1.3					■	■	
	citrate synthase	2.3.3.1/2.3.3.16	■	■	■		■	■	■
	dihydrolipoamide dehydrogenase	1.8.1.4			■	■	■	■	
	fumarate hydratase	4.2.1.2		■	■	■		■	■
	isocitrate dehydrogenase	1.1.1.42					■		
	NADP-dependent isocitrate dehydrogenase	1.1.1.42	■	■	■		■	■	■
	succinate dehydrogenase	1.3.5.1	■		■	■		■	■
	succinate--CoA ligase	6.2.1.5			■	■	■	■	■

Protein export and secretion system

Enzyme secretion	Type 2 SS					■	■	■	
EPS production-associated protein export	Exosortase							■	
Folded protein export	Tat system						■	■	
Inner membrane protein translocation	Sec system				■	■	■	■	■
Toxin secretion	Type 1 SS				■	■			■
Virulence factor secretion/ competition	Type 6 SS					■			■

Redox homeostasis and oxidative stress										
	Oxidative stress	**Peroxiredoxin**								
		Alkyl hydroperoxide reductase	1.11.1.26							
		Catalase	1.11.1.6							
		Disulfide reductase								
		Glutamate--cysteine ligase	6.3.2.2							
		Peroxidase	1.11.1.7							
		Superoxide dismutase	1.15.1.1							
	Redox homeostasis	Glutaredoxin								
		NAD(P) reductase								
	Redox homeostasis and oxidative stress	Thioredoxin								
Stress response										
	Cold stress	**Cold-shock protein**								
	Starvation/stationary phase	**Ribosome-associated translation inhibitor RaiA**								
	Acid stress	BolA family transcriptional regulator								
	Extracytoplasmic stress	Phage shock protein PspA								
		RIP metalloprotease RseP								
		RNA polymerase sigma factor RpoE								
	Fe-S cluster repair	SufS family cysteine desulfurase								
	General stress response	Universal stress protein								
	Heat-shock	Heat-shock protein								
		RNA polymerase sigma factor RpoH								
	Nitrosative stress	Nitric-oxide reductase	1.7.2.5							
		NO-inducible flavohemoprotein								
	Osmotic stress: osmoprotectant	Choline ABC transporter substrate-binding protein								
		Choline dehydrogenase	1.1.99.1							
		Dimethylglycine demethylation protein DgcA								
		Glycine betaine/L-proline ABC transporter ATP-binding protein ProV								
		ProQ/FinO family protein								
		Transcriptional regulator BetI								
	Signal transduction	Symmetrical bis(5-nucleosyl)-tetraphosphatase								
	SOS response	Transcriptional repressor LexA								
	Starvation/ stationary phase	Stringent starvation protein A								
		RNA polymerase sigma factor RpoS								
	Stringent response	Bifunctional (p)ppGpp synthetase/guanosine-3,5-bis								
		GTP diphosphokinase RelA								
		RNA polymerase-binding protein DksA								
	Sugar phosphate stress	Methylglyoxal synthase								
	Toxin/antitoxin	Toxin/antitoxin system								
Sulfur compound metabolism										
	Cysteine degradation	D-cysteine desulfhydrase	4.4.1.15							
	Sulfate reduction	Sulfate adenylyltransferase subunit CysD	2.7.7.4							
		HTH-type transcriptional regulator CysB								
	Sulfite oxidation	Sulfite dehydrogenase	1.8.2.1							
	Sulfite transport	Sulfite exporter TauE/SafE family protein								
	Sulfolactate utilisation	(S)-sulfolactate dehydrogenase	1.1.1.310							
		Sulfoacetaldehyde acetyltransferase	2.3.3.15							
	Sulfur oxidation	Flavocytochrome c sulfide dehydrogenase	1.8.2.3							
	Thiosulfate oxidation	Sulfur oxidation c-type cytochrome SoxA	2.8.5.2							
		Sulfur oxidation protein SoxCD, sulfur dehydrogenase subunit	1.8.2.6							
Virulence/ fitness										
	Toxin production	Putative RTX toxin/ hemolysin								
		Transcriptional activator HlyU								

High metabolic activity, revealed by a series of functional categories, was observed in all genera. In the "Translation" category, genes encoding ribosomal proteins, elongation and initiation factors, and tRNA ligases were overexpressed for all seven genera. In the "Precursor metabolite and energy production and conversion (Energy)" category, genes encoding ATP synthase and enzymes involved in glycolysis/neoglucogenesis and the TCA cycle were systematically present, as were genes encoding proteins of the respiratory chains (e.g. cytochrome-c and cytochrome oxidases). In the "Transcription and RNA metabolism (RNA)" category, genes encoding the various subunits of the RNA polymerase were overexpressed, as was the transcription housekeeping sigma factor RpoD (**Supplementary Table 6**).

Functions important for stress adaptation and resistance to host defenses varied over the course of pathogenesis according to the bacterial genera considered (**Table 1**). "Stress response" genes encoding cold-shock proteins and the ribosome-associated translation inhibitor RaiA were overexpressed by all genera. The gene encoding the stress response RNA polymerase Sigma factor RpoS was overexpressed in members of the Oceanospirillaceae family *(Amphritea Marinobacterium, Marinomonas,* and *Oceanospirillum).* In the "redox homeostasis and oxidative stress" category, peroxiredoxin genes were overexpressed by all genera, along with additional genus-specific functions related to fighting oxidative stress (superoxide dismutases, catalases, and peroxidases) (**Table 1**). In addition, all genera except *Oceanospirillum* overexpressed genes that included several nitrite and nitrate reductases (classified in "Precursor metabolite and energy production and conversion"), hydroxylamine reductases (classified in "Nitrogen compound metabolism"), and nitric-oxide reductase components (classified in "Stress response/ Nitrosative stress"), all of which could contribute to tolerance/resistance to reactive nitrogen species (RNS). RNS, like ROS, are important effectors of oyster immunity [38].

"Cell defense", "Metal homeostasis" and "Virulence/ fitness" categories were more specifically encoded by a subset of bacterial genera. In the "Cell defense" category, multidrug resistance efflux pumps with a TolC component and detoxifying enzymes were overexpressed in some genera. For instance, an outer membrane channel protein TolC was overexpressed up to 16-fold ($\log2(EF) \geq 4$) in *Pseudoalteromonas* (**Supplementary Table 6**). Genes encoding Rhodanese, an enzyme that detoxifies cyanide, were overexpressed in *Marinobacterium*, *Pseudoalteromonas,* and *Vibrio*. Several arsenate reductase genes were also overexpressed in *Marinobacterium, Marinomonas,* and *Pseudoalteromonas*. Genes encoding formaldehyde dehydrogenase, an aldehyde-detoxifying enzyme, were overexpressed in the Oceanospirillaceae. Notably, no cell defense genes were overexpressed in *Arcobacter*. In the "Metal homeostasis" category, 23 of 33 overexpressed genes were involved in iron homeostasis. These genes are mainly expressed by *Marinobacterium* and *Marinomonas*. In *Vibrio*, the only up-regulated gene of the category is annotated as a cobalt/magnesium transporter. In the "Virulence / fitness" category, a small number of overexpressed genes corresponded to putative toxins encoded by

Arcobacter, *Oceanospirillum*, *Pseudoalteromonas*, and *Vibrio*. This has to be completed by genes from the "Protein export and secretion system" category, which are important for both virulence and interbacterial competitions. Genes encoding the general protein export system (i.e. the "Sec" system of Gram-negative bacteria [39, 40]) were overexpressed by all genera, while type VI secretion systems were overexpressed specifically in *Vibrio* (e.g. *V. crassostreae*) and *Marinomonas*.

Finally, a global increase in the "Sulfur compound metabolism" category was observed in *Marinobacterium* (**Figure 5**). Overexpressed proteins of this category were also found in other genera (**Table 1** and **Supplementary Table 6**). Interestingly, these overexpressed proteins corresponded to enzymes that were (mostly non-redundantly) encoded by five different genera. Altogether, these enzymes constitute several sulfur metabolic pathways (**Figure 6**).

These results highlight functional complementation at the level of the bacterial community, and a metabolic adaptation to the within-host environment, both of which are likely important for successful oyster colonization.

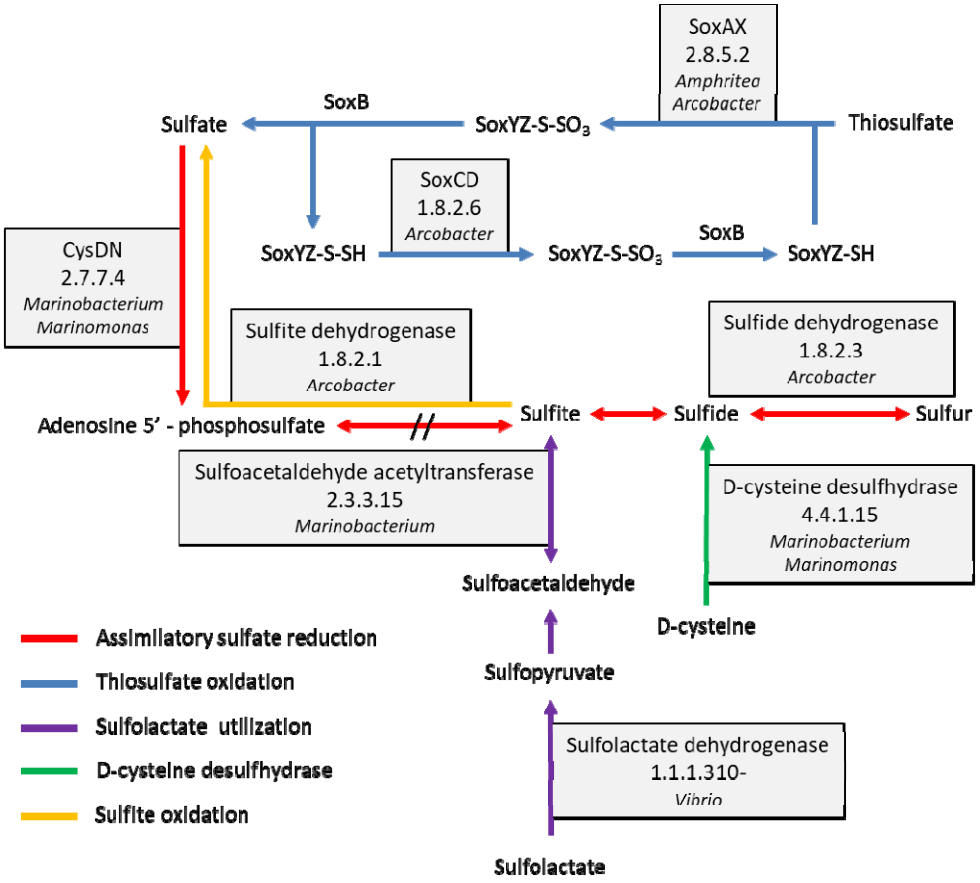

Figure 6: Integrated sulfur cycle in the diseased oyster microbiota. Overexpressed sulfur metabolism pathways are shown. Enzymatic reactions are represented by arrows that are colored according to the pathway. The Enzyme Commission (E.C.) number, corresponding gene name, and genera overexpressing the gene for the enzyme catalyzing each reaction is provided in the grey rectangle beside the relevant arrow.

DISCUSSION

In this study, we have shown that the dysbiosis associated with POMS is conserved across infectious environments. Using metabarcoding, we demonstrated that diseased oysters affected by POMS are colonized by a common consortium of bacteria comprising ten major genera (*Arcobacter*, *Cryomorphaceae*, *Marinobacterium*, *Marinomonas*, *Proxilibacter*, *Pseudoalteromonas*, *Psychrilyobacter*, *Psychrobium*, *Psychromonas*, and *Vibrio*). Using metatranscriptomics, we showed that five of these genera (*Arcobacter*, *Marinobacterium*, *Marinomonas*, *Vibrio*, and *Pseudoalteromonas)* were particularly transcriptionally active.

The bacterial consortium associated with POMS was remarkably similar in three different susceptible oyster families and two different environments. All diseased oyster families harbored similar microbial communities, with only a few exceptions. Remarkably, the oyster-associated microbial communities were conserved across infectious environments, although the Mediterranean and Atlantic ecosystems are likely to host diverse bacterial communities.

Until recently, only members of the *Vibrio* genus had been repeatedly associated with POMS. These studies used culture-based approaches to investigate oyster-associated bacterial communities (Lemire et al., 2015; Bruto et al., 2018). *Vibrio* species associated with POMS were characterized by key virulence factors that are required to weaken oyster cellular defenses (Rubio et al., 2019; Piel et al., 2019). Members of the *Arcobacter* genus had also been associated with POMS-diseased oysters [41, 42], but the role of this genus in pathogenesis was not investigated more deeply due to limitations of culture-based techniques [43]. In the present study, we extended the core colonizing microbiota to five bacterial genera. The discovery of the contributions of these genera, which are responsible for up to 40% of the bacterial transcriptional activity observed in POMS, provides new insights into the pathogenesis of POMS. Altogether, our results strongly suggest that a colonizing core microbiota, rather than specific bacterial pathogens, operates as a functional unit of pathogenesis. Together with OsHV-1, these bacteria form the POMS pathobiota. POMS secondary bacteremia may resemble periodontitis in humans, in which the evolution of the disease is characterized by the development of a pathogenic consortium comprising a limited number of species [44, 45].

We used metatranscriptomics to unveil the functions of the microbiota in relation to POMS. Bacterial metatranscriptomics from host tissues is technically challenging (due to the low proportion of bacterial transcripts in the host samples), but it provides functional information that is thought to more accurately portray the role of the microbiota in health and disease states [46]. Accordingly, gene expression profiling has proven highly successful in advancing the understanding of the dynamics of disease-associated microbial populations [47]. In the case of POMS, by linking functional genes to the bacterial genera which encode them, we found a remarkably consistent relationship between the structure of bacterial communities (through 16S metabarcoding) and the functions expressed by

bacterial genera in the communities (through metatranscriptomics), further supporting our hypothesis of a pathobiota composed of at least five key genera.

Among functions overexpressed in the diseased oyster-associated microbiota, we first identified core functions which were overrepresented in all dominant genera (**Table 1**). In addition to housekeeping functions with expression levels that reflect the rapid growth of the genus (e.g. translation and transcription, central metabolism), we found functional redundancy in two important categories required for adaptation to the within-host environment: stress response and redox homeostasis.

We found a systematic and important overproduction of various cold shock proteins in the "Stress response" functional category (**Supplementary Table 6**). In the diseased oyster microbiota, these proteins may be important to sustain the high level of transcription and translation we observed [48, 49]. Redox homeostasis was another core function. Fighting oxidative stress in the host can be crucial to survival and multiplication within the host. Thus, bacteria have many lines of defense against oxidative damage [50]. Key enzymes and proteins involved in redox homeostasis and oxidative stress response were overexpressed in several of the five genera, including superoxide dismutases (which catalyze the dismutation of superoxide in hydrogen peroxide) and catalases and peroxidases (which destroy hydrogen peroxide and other toxic peroxide compounds). All five genera overexpressed redoxin, a small redox protein which plays important roles in maintaining an intracellular reducing environment, and also acts as a cofactor in intracellular oxidoreductase reactions. Other proteins important for fighting oxidative stress were specific to one or more given genera. For example, NAD(P) reductase (which contributes to the homeostasis of reduced NAD(P)H, an important source of reducing potential) was enriched in *Amphitrea*, *Marinobacterium*, *Marinomonas*, and *Oceanospirillum*, four members of the Oceanospirillaceae family. Glutamate – cysteine ligase (which is responsible for the production of Glutathione, an important antioxidant compound, and is also involved in detoxifying reactions) was overexpressed in *Amphitrea*, *Oceanospirillum*, and *Pseudoalteromonas*. Earlier functional studies have identified the AhpCF complex detoxifying enzyme alkylhydroxyperoxydase as a key determinant of resistance to ROS and thus oyster

colonization in *Vibrio* [51]. In the diseased oyster microbiota, this enzyme was over-produced in *Marinomonas* and *Oceanospirillum*. All of the successful genera, except *Oceanospirillum*, also expressed enzymes required for tolerance/resistance to RNS (**Table 1**). ROS and RNS are major players at the oyster-microbiota interface (Destoumieux-Garzon et al., 2020), thus it is not surprising that successful colonizers express ROS detoxifying enzymes during oyster colonization. In summary, each genus overexpressed several proteins involved in stress response, especially oxidative stress, although each genus had its own repertoire of proteins.

We found that the bacterial community associated with POMS also expresses a series of genus-specific (variable) functions. These functions include adhesion, cell defense, cell motility, metal homeostasis, natural competence, quorum sensing, sulfur metabolism, transport, and virulence (**Table 1**). The observation that functions of interest may be contributed by a single or multiple bacterial genera within a microbial community has also been made in the human gut [46, 52]. Interestingly, a function expressed by one genus can be useful for the community as a whole. Functional complementarity within the oyster-associated microbiota may therefore contribute to synergy between genera.

Evidence of cross-benefits at the community level in the oyster microbiota was found in the form of overexpressed genes related to iron homeostasis (**Supplementary Table 6**). The capacity to scavenge iron from the environment and the host is a well-known determinant of pathogenicity [53, 54]. Except for *Vibrio*, all genera overexpressed functions related to iron acquisition (e.g. iron siderophore production and transport, which enable the chelation and uptake of iron). However, in the consortium, only *Marinomonas* and *Marinobacterium* expressed siderophore-production enzymes, while other members of the microbiota expressed the receptors for iron-siderophore uptake. Similarly, virulence factors (such as secreted RTX family toxins) were expressed by *Vibrio* and *Arcobacter*, while the Type 6 Secretion System (T6SS) was expressed by *Vibrio* and *Marinomonas*. T6SS expressed by *Vibrio* has been shown to contribute to the suppression of oyster cellular defenses [21, 55]. Therefore, their expression by a few genera is likely beneficial to the whole pathobiota.

547 The best example of cross-benefits, however, is the "Sulfur compound metabolism" functional
548 category. Marine *Arcobacter* species that can oxidize sulfide to elemental sulfur, producing sulfur
549 filaments, have been previously identified [56]. In our consortium, corresponding sulfide
550 dehydrogenase enzymatic activity (E.C. 1.8.2.3) was encoded by *Arcobacter* only, while other sulfur
551 compound metabolic pathways were associated with four other genera (mostly *Marinomonas* and
552 *Marinobacterium*) (**Figure 6**). This suggests that sulfur cycling is a property of the colonizing core
553 microbiota as a whole, and not of a single genus. A similar association between *Arcobacter* and
554 *Marinobacter* species has been described in biogeochemical cycling, specifically in the environment
555 of natural gas wells [57]. We believe that such interdependence and cooperation within microbial
556 communities allows these communities to meet metabolic requirements and mount an efficient stress
557 response, which are key determinants of their success. We further believe that this helps to explain the
558 conserved pathobiota structure associated with POMS across distinct environments and oyster genetic
559 backgrounds.

560

561 **Supplementary Materials**

562 Supplementary Table 1: Total raw reads (R1+R2) at each stage of biocomputing, after sequencing and
563 removal of rRNA reads (eukaryotic and bacterial), oyster reads, and viral reads.

564 Supplementary Table 2: List of functional categories defined in bacterial metatranscriptomics.

565 Supplementary Table 3: Complete list of contigs identified in bacterial metatranscriptomics, with
566 annotations and expression value in TPM. Taxons in red correspond to assignation at taxonomic ranks
567 other than the genus level.

568 Supplementary Table 4: Absolute abundance of Operational Taxonomic Units (*ie.* clusters) and their
569 corresponding taxonomic affiliations in susceptible and resistant oyster families confronted with two
570 different infectious environments. Susceptible oyster families are S_{F11}, S_{F14}, and S_{F15}; resistant oyster
571 families are R_{F21}, R_{F23}, and R_{F48}. A indicates the Atlantic infectious environment, M the Mediterranean

572 infectious environment. T0, T6, T12, T24, T48, T60, and T72 indicate sampling times (in hours) over
573 the course of experimental infection. R1, R2, R3 indicate the results of each replicate (Excel file).

574 Supplementary Table 5: Frequencies of bacterial taxa that change significantly in abundance over the
575 course of each experimental infection (Atlantic or Mediterranean) in susceptible and resistant oyster
576 families. The change in abundance of bacterial taxa between initial and final time points was
577 determined using DEseq2 with the adjusted p-value < 0.05. Susceptible oyster families are SF11,
578 SF14, and SF15; resistant oyster families are RF21, RF23, and RF48. A indicates the Atlantic
579 infectious environment, M the Mediterranean infectious environment. T0, T6, T12, T24, T48, T60
580 and T72 indicate sampling times (in hours) over the course of experimental infection. R1, R2, R3
581 indicate the results of each replicate (Excel file).

582 Supplementary Table 6: List of the overexpressed (enriched) proteins in the seven main genera found
583 to colonize diseased oysters. A protein was considered enriched when it had a log2(EF) $\geq$ 1 with a p-
584 value $\leq$ 0.05 (Student's t-test) in at least two conditions.

585 Supplementary Figure 1: Schematic representation of the steps of metatranscriptomic data analysis.

586 Supplementary Figure 2: Rarefaction curves of the sub-sampled 16S rDNA dataset (10,000 reads per
587 sample) for susceptible and resistant oysters in (a) the Atlantic infectious environment (AS_{F11}, AS_{F14},
588 AS_{F15} and AR_{F21}, AR_{F23}, $AR_{F48)}$ and (b) the Mediterranean infectious environment (MS_{F11}, MS_{F14},
589 MS_{F15} and MR_{F21}, MR_{F23}, MR_{F48}). T0, T6, T12, T24, T48, T60, and T72 indicate sampling times (in
590 hours) over the course of experimental infection. Results are shown in triplicate for each time point.
591 Supplementary Figure 3: Microbiota modification as analysed using 16S rDNA metabarcoding in
592 susceptible and resistant oyster families confronted with two different infectious environments.
593 Susceptible oyster families (S_{F11}, S_{F14} and S_{F15}) and resistant oyster families (R_{F21}, R_{F23} and R_{F48})
594 confronted with (**a**) Atlantic or (**b**) Mediterranean infectious environments. Significant changes in
595 abundance (up or down; DESeq2, p-value < 0.05) between the initial and the final time point of the
596 infection were much greater for each taxonomic rank (from the phylum to the OTU rank) for
597 susceptible oyster families than for resistant oyster families. Data for AS_{F11} and AR_{F21} were extracted

598 from [20].

599 Supplementary Figure 4: Heatmaps of bacterial communities that changed significantly in abundance
600 over the course of infection in resistant oysters (R_{F11}, R_{F14}, R_{F15}) in the Atlantic and Mediterranean
601 infectious environments. Analyses were performed at the genus level. Only genera with a relative
602 proportion greater than 2% in at least one sample are shown. Increased color intensity (blue) indicates
603 increased relative abundance of the genus.

604

605 **END NOTES**

606 **Acknowledgements.** We warmly thank the staff of the Ifremer stations of Argenton (LPI, PFOM) and
607 Sète (LER), and the Comité Régional de Conchyliculture de Méditerranée (CRCM) for technical
608 support in the collection of the oyster genitors and reproduction of the oysters. The authors are grateful
609 to Philippe Clair from the qPHD platform/Montpellier genomix for useful advice. This work benefited
610 from the support of the National Research Agency under the "Investissements d'avenir" program
611 (reference ANR-10-LABX-04-01) through use of the GENSEQ platform (http://www.labex-
612 cemeb.org/fr/genomique-environnementale-2) from the labEx CeMEB. The present study was
613 supported by the ANR projects DECIPHER (ANR-14-CE19-0023) and DECICOMP (ANR-19-CE20-
614 0004), and by Ifremer, CNRS, Université de Montpellier and Université de Perpignan *via* Domitia.
615 This study is set within the framework of the "Laboratoires d'Excellence (LABEX)" TULIP
616 (ANR□10□LABX□41).

617

618 **Author contributions**

619 J.D.L., B.P., A.J. and G.M. designed experiments. B. P., J.D.L, A.L., J.M.E., Y.G., L.D. and G.M.
620 performed oyster experiments. J.D.L., A.L., E.T., C.C and G.M. performed microbiota analyses.
621 J.D.L. and A.L. performed qPCR analyses. A.J. and X.L performed the metatranscriptomic
622 experiments. A.J. and S.M. analyzed the metatranscriptomic data. J.D.L., A.L., A.J, S.M. and G.M.
623 interpreted results. J.D.L., A.L., A.J., D. D. G. and G.M. wrote the manuscript, which has been
624 reviewed and approved by all authors.

625

626 **Conflict of interest statement.** There are no conflicts of interest. This manuscript represents original

627 results, and has not been submitted elsewhere for publication.

628

629 REFERENCES

630

631 1. EFSA: P. o. A. H. W. Oyster mortality. *EFSA Journal* 2015, 13(4122-n/a).
632 2. Paul-Pont I, Dhand NK, Whittington RJ: Influence of husbandry practices on OsHV-1
633 associated mortality of Pacific oysters Crassostrea gigas. *Aquaculture* 2013, 412:202-214.
634 3. Martenot C, Oden E, Travaille E, Malas JP, Houssin M: Detection of different variants of
635 Ostreid Herpesvirus 1 in the Pacific oyster, Crassostrea gigas between 2008 and 2010. *Virus*
636 *Res* 2011, 160(1-2):25-31.
637 4. Renault T, Moreau P, Faury N, Pepin JF, Segarra A, Webb S: Analysis of clinical ostreid
638 herpesvirus 1 (Malacoherpesviridae) specimens by sequencing amplified fragments from
639 three virus genome areas. *J Virol* 2012, 86(10):5942-5947.
640 5. Segarra A, Pepin JF, Arzul I, Morga B, Faury N, Renault T: Detection and description of a
641 particular Ostreid herpesvirus 1 genotype associated with massive mortality outbreaks of
642 Pacific oysters, Crassostrea gigas, in France in 2008. *Virus Res* 2010, 153(1):92-99.
643 6. Peeler EJ, Reese RA, Cheslett DL, Geoghegan F, Power A, Thrush MA: Investigation of
644 mortality in Pacific oysters associated with Ostreid herpesvirus-1 muVar in the Republic of
645 Ireland in 2009. *Prev Vet Med* 2012, 105(1-2):136-143.
646 7. Lynch SA, Carlsson J, Reilly AO, Cotter E, Culloty SC: A previously undescribed ostreid herpes
647 virus 1 (OsHV-1) genotype detected in the pacific oyster, Crassostrea gigas, in Ireland.
648 *Parasitology* 2012, 139(12):1526-1532.
649 8. EFSA PoAHW: Oyster mortality. *EFSA Journal* 2015, 13(6):4122-n/a.
650 9. Abbadi M, Zamperin G, Gastaldelli M, Pascoli F, Rosani U, Milani A, Schivo A, Rossetti E,
651 Turolla E, Gennari L *et al*: Identification of a newly described OsHV-1 microvar from the North
652 Adriatic Sea (Italy). *J Gen Virol* 2018, 99(5):693-703.
653 10. Burioli EAV, Prearo M, Houssin M: Complete genome sequence of Ostreid herpesvirus type 1
654 microVar isolated during mortality events in the Pacific oyster Crassostrea gigas in France
655 and Ireland. *Virology* 2017, 509:239-251.
656 11. Burioli EAV, Prearo M, Riina MV, Bona MC, Fioravanti ML, Arcangeli G, Houssin M: Ostreid
657 herpesvirus type 1 genomic diversity in wild populations of Pacific oyster Crassostrea gigas
658 from Italian coasts. *J Invertebr Pathol* 2016, 137:71-83.
659 12. Azéma P, Lamy JB, Boudry P, Renault T, Travers MA, Dégremont L: Genetic parameters of
660 resistance to Vibrio aestuarianus, and OsHV-1 infections in the Pacific oyster, Crassostrea
661 gigas, at three different life stages. *Genetics Selection Evolution* 2017, 49:1-16.
662 13. Le Roux F, Wegner KM, Polz MF: Oysters and Vibrios as a Model for Disease Dynamics in Wild
663 Animals. *Trends Microbiol* 2016, 24(7):568-580.
664 14. Pernet F, Barret J, Le Gall P, Corporeau C, Dégremont L, Lagarde F, Pépin JF, Keck N: Mass
665 mortalities of Pacific oysters Crassostrea gigas reflect infectious diseases and vary with
666 farming practices in the Mediterranean Thau lagoon, France. *Aquaculture Environment*
667 *Interactions* 2012, 2(3):215-237.
668 15. Pernet F, Barret J, Marty C, Moal J, Le Gall P, Boudry P: Environmental anomalies, energetic
669 reserves and fatty acid modifications in oysters coincide with an exceptional mortality event.

Marine Ecology Progress Series 2010, 401:129-146.

16. Pernet F, Tamayo D, Fuhrmann M, Petton B: Deciphering the effect of food availability, growth and host condition on disease susceptibility in a marine invertebrate. *J Exp Biol* 2019, 222(Pt 17).
17. Petton B, Pernet F, Robert R, Boudry P: Temperature influence on pathogen transmission and subsequent mortalities in juvenile Pacific oysters Crassostrea gigas. *Aquaculture Environment Interactions* 2013, 3(3):257-273.
18. Bruto M, James A, Petton B, Labreuche Y, Chenivesse S, Alunno-Bruscia M, Polz MF, Le Roux F: Vibrio crassostreae, a benign oyster colonizer turned into a pathogen after plasmid acquisition. *ISME J* 2017, 11(4):1043-1052.
19. Lemire A, Goudenege D, Versigny T, Petton B, Calteau A, Labreuche Y, Le Roux F: Populations, not clones, are the unit of vibrio pathogenesis in naturally infected oysters. *ISME J* 2015, 9(7):1523-1531.
20. de Lorgeril J, Lucasson A, Petton B, Toulza E, Montagnani C, Clerissi C, Vidal-Dupiol J, Chaparro C, Galinier R, Escoubas JM *et al*: Immune-suppression by OsHV-1 viral infection causes fatal bacteraemia in Pacific oysters. *Nat Commun* 2018, 9(1):4215.
21. Rubio T, Oyanedel D, Labreuche Y, Toulza E, Luo X, Bruto M, Chaparro C, Torres M, de Lorgeril J, Haffner P *et al*: Species-specific mechanisms of cytotoxicity toward immune cells determine the successful outcome of Vibrio infections. *Proc Natl Acad Sci U S A* 2019, 116(28):14238-14247.
22. de Lorgeril J, Petton B, Lucasson A, Perez V, Stenger PL, Degremont L, Montagnani C, Escoubas JM, Haffner P, Allienne JF *et al*: Differential basal expression of immune genes confers Crassostrea gigas resistance to Pacific oyster mortality syndrome. *BMC Genomics* 2020, 21(1):63.
23. Petton B, Boudry P, Alunno-Bruscia M, Pernet F: Factors influencing disease-induced mortality of Pacific oysters Crassostrea gigas. *Aquaculture Environment Interactions* 2015, 6(3):205-222.
24. Pfaffl MW: A new mathematical model for relative quantification in real-time RT-PCR. *Nucleic Acids Res* 2001, 29(9):e45.
25. Klindworth A, Pruesse E, Schweer T, Peplies J, Quast C, Horn M, Glockner FO: Evaluation of general 16S ribosomal RNA gene PCR primers for classical and next-generation sequencing-based diversity studies. *Nucleic Acids Res* 2013, 41(1):e1.
26. Escudie F, Auer L, Bernard M, Mariadassou M, Cauquil L, Vidal K, Maman S, Hernandez-Raquet G, Combes S, Pascal G: FROGS: Find, Rapidly, OTUs with Galaxy Solution. *Bioinformatics* 2017, 34(8):1287-1294.
27. Magoc T, Salzberg SL: FLASH: fast length adjustment of short reads to improve genome assemblies. *Bioinformatics* 2011, 27(21):2957-2963.
28. Mahe F, Rognes T, Quince C, de Vargas C, Dunthorn M: Swarm: robust and fast clustering method for amplicon-based studies. *PeerJ* 2014, 2:e593.
29. Rognes T, Flouri T, Nichols B, Quince C, Mahe F: VSEARCH: a versatile open source tool for metagenomics. *PeerJ* 2016, 4:e2584.
30. Langmead B, Salzberg SL: Fast gapped-read alignment with Bowtie 2. *Nat Methods* 2012, 9(4):357-359.
31. Rosani U, Shapiro M, Venier P, Allam B: A Needle in A Haystack: Tracing Bivalve-Associated Viruses in High-Throughput Transcriptomic Data. *Viruses* 2019, 11(3).
32. Buchfink B, Xie C, Huson DH: Fast and sensitive protein alignment using DIAMOND. *Nat Methods* 2015, 12(1):59-60.
33. Huson DH, Albrecht B, Bagci C, Bessarab I, Gorska A, Jolic D, Williams RBH: MEGAN-LR: new algorithms allow accurate binning and easy interactive exploration of metagenomic long reads and contigs. *Biol Direct* 2018, 13(1):6.
34. Anders S, Pyl PT, Huber W: HTSeq--a Python framework to work with high-throughput sequencing data. *Bioinformatics* 2015, 31(2):166-169.

35. team RC: R: a language and environment for statistical computing. In.: R Foundation for Statistical Computing; 2013.
36. Love MI, Huber W, Anders S: Moderated estimation of fold change and dispersion for RNA-seq data with DESeq2. *Genome Biol* 2014, 15(12):550.
37. McMurdie PJ, Holmes S: phyloseq: an R package for reproducible interactive analysis and graphics of microbiome census data. *PLoS One* 2013, 8(4):e61217.
38. Destoumieux-Garzon D, Canesi L, Oyanedel D, Travers MA, Charriere GM, Pruzzo C, Vezzulli L: Vibrio-bivalve interactions in health and disease. *Environ Microbiol* 2020.
39. Smets D, Loos MS, Karamanou S, Economou A: Protein Transport Across the Bacterial Plasma Membrane by the Sec Pathway. *Protein J* 2019, 38(3):262-273.
40. Beckwith J: The Sec-dependent pathway. *Res Microbiol* 2013, 164(6):497-504.
41. Lasa A, di Cesare A, Tassistro G, Borello A, Gualdi S, Furones D, Carrasco N, Cheslett D, Brechon A, Paillard C *et al*: Dynamics of the Pacific oyster pathobiota during mortality episodes in Europe assessed by 16S rRNA gene profiling and a new target enrichment next-generation sequencing strategy. *Environ Microbiol* 2019, 21(12):4548-4562.
42. Lokmer A, Mathias Wegner K: Hemolymph microbiome of Pacific oysters in response to temperature, temperature stress and infection. *ISME J* 2015, 9(3):670-682.
43. Rahman FU, Andree KB, Salas-Masso N, Fernandez-Tejedor M, Sanjuan A, Figueras MJ, Furones MD: Improved culture enrichment broth for isolation of Arcobacter-like species from the marine environment. *Sci Rep* 2020, 10(1):14547.
44. Yost S, Duran-Pinedo AE, Teles R, Krishnan K, Frias-Lopez J: Functional signatures of oral dysbiosis during periodontitis progression revealed by microbial metatranscriptome analysis. *Genome Med* 2015, 7(1):27.
45. Lamont RJ, Hajishengallis G: Polymicrobial synergy and dysbiosis in inflammatory disease. *Trends Mol Med* 2015, 21(3):172-183.
46. Heintz-Buschart A, Wilmes P: Human Gut Microbiome: Function Matters. *Trends Microbiol* 2018, 26(7):563-574.
47. Murray JL, Connell JL, Stacy A, Turner KH, Whiteley M: Mechanisms of synergy in polymicrobial infections. *J Microbiol* 2014, 52(3):188-199.
48. Phadtare S: Unwinding activity of cold shock proteins and RNA metabolism. *RNA Biol* 2011, 8(3):394-397.
49. Phadtare S, Severinov K: RNA remodeling and gene regulation by cold shock proteins. *RNA Biol* 2010, 7(6):788-795.
50. Staerck C, Gastebois A, Vandeputte P, Calenda A, Larcher G, Gillmann L, Papon N, Bouchara JP, Fleury MJJ: Microbial antioxidant defense enzymes. *Microb Pathog* 2017, 110:56-65.
51. Vanhove AS, Rubio TP, Nguyen AN, Lemire A, Roche D, Nicod J, Vergnes A, Poirier AC, Disconzi E, Bachere E *et al*: Copper homeostasis at the host vibrio interface: lessons from intracellular vibrio transcriptomics. *Environ Microbiol* 2016, 18(3):875-888.
52. Schirmer M, Franzosa EA, Lloyd-Price J, McIver LJ, Schwager R, Poon TW, Ananthakrishnan AN, Andrews E, Barron G, Lake K *et al*: Dynamics of metatranscription in the inflammatory bowel disease gut microbiome. *Nat Microbiol* 2018, 3(3):337-346.
53. Begg SL: The role of metal ions in the virulence and viability of bacterial pathogens. *Biochem Soc Trans* 2019, 47(1):77-87.
54. Lemos ML, Balado M: Iron uptake mechanisms as key virulence factors in bacterial fish pathogens. *J Appl Microbiol* 2020, 129(1):104-115.
55. Piel D, Bruto M, James A, Labreuche Y, Lambert C, Janicot A, Chenivesse S, Petton B, Wegner KM, Stoudmann C *et al*: Selection of Vibrio crassostreae relies on a plasmid expressing a type 6 secretion system cytotoxic for host immune cells. *Environ Microbiol* 2019.
56. Wirsen CO, Sievert SM, Cavanaugh CM, Molyneaux SJ, Ahmad A, Taylor LT, DeLong EF, Taylor CD: Characterization of an autotrophic sulfide-oxidizing marine Arcobacter sp. that produces filamentous sulfur. *Appl Environ Microbiol* 2002, 68(1):316-325.
57. Evans MV, Panescu J, Hanson AJ, Welch SA, Sheets JM, Nastasi N, Daly RA, Cole DR, Darrah

774 TH, Wilkins MJ *et al*: Members of Marinobacter and Arcobacter Influence System
775 Biogeochemistry During Early Production of Hydraulically Fractured Natural Gas Wells in the
776 Appalachian Basin. *Front Microbiol* 2018, 9:2646.
777